

Colloidal quantum dot solar cells

Edward H. Sargent

Solar cells based on solution-processed semiconductor nanoparticles — colloidal quantum dots — have seen rapid advances in recent years. By offering full-spectrum solar harvesting, these cells are poised to address the urgent need for low-cost, high-efficiency photovoltaics.

Although the Sun supplies the Earth with enough energy in one hour to meet global electricity needs for one year, solar-generated electricity today supplies only around 0.1% of worldwide demand. Efficient, robust solar cells can be made, proving that no fundamental obstacle exists to meeting an appreciable portion of our energy needs from solar-generated electricity.

What is required now is a major advance in engineering. We must build a technology for harvesting solar energy that does not compromise between the simultaneous goals of high efficiency and low cost. A single figure of merit captures this requirement: if solar energy harvesting is achieved at an installed cost of \$1 per watt-peak (W_p), then it will produce electricity over its lifetime at an equivalent cost of around \$0.05 kWh^{-1} , which is compellingly competitive with grid prices¹. This is a purely economic advantage that requires no subsidies to compete in the open market and does not even begin to consider the important environmental benefits of solar power.

The price of a solar module represents around half the cost of an installed solar-energy-producing system. The rest of the cost comes from the inverter, racking and electrical hardware. Reducing the cost of solar modules and increasing efficiencies are both ways to lower the cost of the final system. The following equation provides a breakdown of the overall cost per watt-peak, given that the Sun provides a peak illumination of $1,000 W_p m^{-2}$:

$$c_{\text{installed}} (W_p^{-1}) = \frac{c_{\text{module}} (m^{-2}) + c_{\text{BOS}} (m^{-2})}{CE (\%) \times 1,000 W_p m^{-2}}$$

where CE is the conversion efficiency, and c_{module} , c_{BOS} and $c_{\text{installed}}$ are the cost per watt-peak of the installed system, the cost per

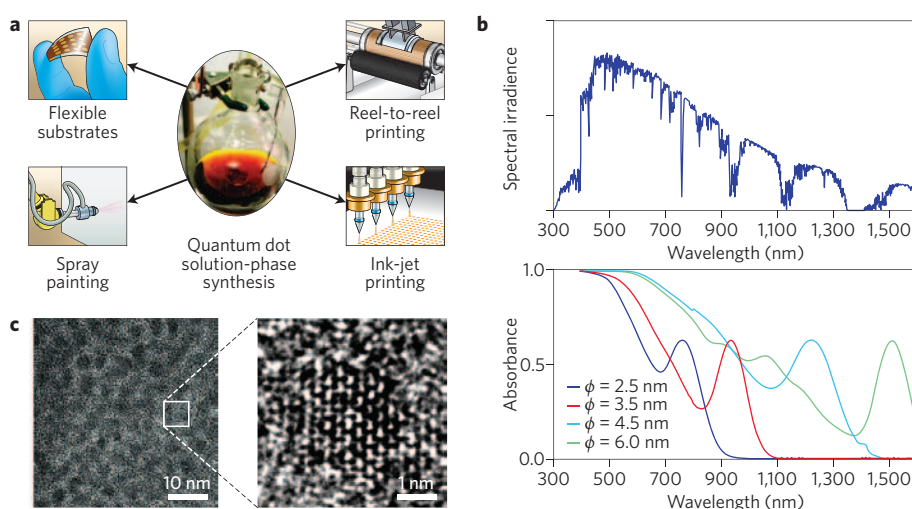


Figure 1 | Solution-processed quantum dot solar cells. **a**, After synthesis, the colloidal quantum dots are deposited onto a flexible substrate at low temperature. Processing techniques for achieving this include spin-coating, spray-coating, reel-to-reel printing and ink-jet printing. **b**, The absorption spectrum of a colloidal quantum dot film (bottom) is readily matched to the power spectrum of the Sun reaching the Earth (top). Nanoparticles with a short-wavelength infrared bandgap can be shifted to blue wavelengths at the synthesis stage by ensuring that they have dimensions on the order of (or smaller than) the Bohr exciton radius (ϕ) characteristic of their constituent semiconductor material. **c**, Colloidal quantum dots that are single-crystalline and substantially monodispersed (same diameter and shape) make up each junction of a single- or multijunction solar cell. Transmission electron microscopy shows both their monodispersed (left) and crystalline (right) nature.

area of the module and the cost per area of the balance of systems, respectively.

The goal of lower module costs is being pursued by constructing solar cells on flexible substrates and employing semiconductors and conductors that can be applied from the liquid phase and at low temperatures (Fig. 1a). Flexible, lightweight substrates offer additional advantages such as lowering the solar module weight, which reduces installation costs.

Quantum tuning

Increasing the efficiency of a solar module lowers the cost contributions, per watt, from

both the module and the balance-of-systems components. Given the practical limitations associated with reducing balance-of-systems costs, it is widely believed that a long-term viable solar technology — even one with an unprecedentedly low module cost — must offer a clear roadmap to achieving power-conversion efficiencies of more than 20%.

Achieving high efficiency demands the effective use of the Sun's broad spectrum (Fig. 1b). Half of the Sun's energy reaching the Earth lies in the visible band, while the other half is in the infrared range. If a single light-absorbing semiconductor is employed in a solar module, its bandgap must lie

in the near-infrared (around 1.1–1.4 eV) to offer a theoretical limit of 31% under unconcentrated illumination conditions.

The Sun's visible and infrared radiation can be more efficiently harnessed if a number of different light-absorbing materials are employed in series. In such a multijunction solar cell, a stack of semiconductors, chirped through the visible to the infrared range, capture not only the abundant energy available in each visible photon, but also the considerable photon current available in the short-wavelength infrared photons, which ordinarily would not be absorbed in a single-junction device. This strategy enables theoretical efficiencies in the range of 40–60%, depending on the number of junctions employed².

Until recently, this approach has been pursued by redesigning the material composition of each active layer³. However, researchers have recently developed a vastly simpler approach that involves tuning via the quantum size effect.

Colloidal quantum dots⁴ (Fig. 1c) are semiconductor nanoparticles synthesized in and processed into thin films from the liquid phase. When the diameter of such a particle is reduced below the characteristic dimensions of electron and hole wavefunctions in the constituent semiconductor material, its energy levels are shifted into the bands of the bulk medium. The absorption spectrum is widely tunable through this effect, as can be seen in Fig. 1b. Modest modifications to synthesis conditions at the time of nanoparticle fabrication enable systematic tuning of the bandgap. Materials systems that have bulk bandgaps smaller than the lowest infrared bandgap of interest in a multijunction cell (0.7 eV in the triple-junction case) and a large exciton Bohr radius (5 nm and above) are ideal candidates. Pb(S, Se, Te), In(Sb, As), SnS and FeS₂ are a few promising examples based on abundant materials⁵.

Colloidal quantum dot devices

Since the first reports of infrared colloidal quantum dot solar cells in 2005⁶, much progress has been made towards technologically relevant efficiencies. When a single-junction power-conversion efficiency of 10% is eventually reached, the multijunction strategy can be deployed to engineer these low-cost, flexible materials into devices with efficiencies of 15%. The latest published reports show single-junction efficiencies of 6%, and progress shows no signs of abating (Fig. 2b).

Colloidal quantum dot films form the core of these devices (Fig. 2a). The film absorbs light to produce an electron–hole pair, which must then be separated

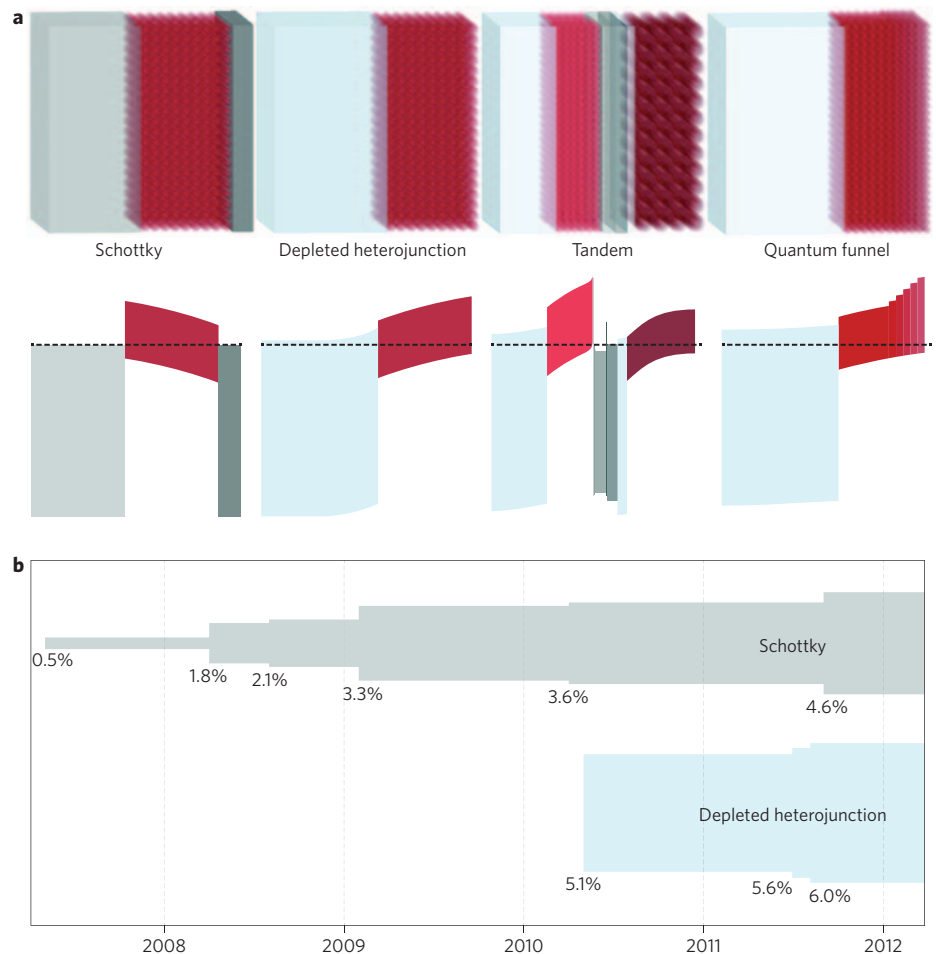


Figure 2 | Optoelectronic device architecture as a driver of colloidal quantum dot solar cell performance. **a**, There have been multiple generations of colloidal quantum dot solar cells: the Schottky device, which employs a metal–semiconductor work function to generate a charge-separating depletion region in the semiconductor layer; the depleted-heterojunction device, which forms an electron-accepting, hole-blocking heterojunction on the illuminated (front) side of the device; the tandem cell, which exploits a size-effect tuning of the bandgap; and the quantum funnel device, which employs quantum tuning to drive minority carriers to the point of extraction. **b**, Progress in power-conversion efficiency for the Schottky and depleted-heterojunction architectures.

and extracted at opposite electrodes. A simple conceptual model that treats colloidal quantum dot films as an effective semiconductor medium — one having average mobilities for electrons and holes, free carrier densities and a dielectric constant — has provided useful guidance in the engineering of both films and devices.

The Schottky cell was the first colloidal quantum dot solar structure to achieve efficiencies of 1%^{7–9}. In this device, a transparent conducting oxide with a relatively large work function, such as indium tin oxide (ITO), forms an Ohmic contact with a p-type colloidal quantum dot film. On the back side of the device, a shallow-work-function metal such as aluminium or magnesium establishes a charge-separating junction to extract

electrons and repel holes. In this depletion region, charge separation is promoted by the built-in field, which enables the rate of carrier withdrawal through transport to outpace that of recombination¹⁰, thus leading to internal quantum efficiencies of more than 80%.

In the quasi-charge-neutral region outside of the depletion region, minority carriers rely on diffusion. Here, transport lengths have been observed to be in the range of 10–100 nm (ref. 11). Schottky devices with an opaque back contact, although attractively simple, fail to scale to active-layer thicknesses of more than 200 nm; beyond this threshold, absorption increases but charge-pair generation occurs too far from the junction to achieve efficient carrier extraction, and thus the internal

quantum efficiency declines. Nevertheless, good progress in efficiency has been achieved through advances in the electronic properties of the colloidal quantum dot film, leading to improvements from 2% in 2008¹² to around 3% in 2009–2010^{13,14}, and now to a recent Schottky cell record of 4.6%¹⁵.

In 2010, researchers reported an architecture that successfully addressed the principal limitation of the Schottky cell¹⁶. The depleted heterojunction colloidal quantum dot solar cell implements charge separation at the front side of the cell via a junction between the active layer and a large-bandgap shallow-work-function electron acceptor. The electron affinity of the electron acceptor is designed to favour electron extraction without compromising the open-circuit voltage¹⁷. The Ohmic contact on the back side also plays a crucial role, and, especially when large-bandgap colloidal quantum dots are employed, requires the use of a large-work-function electrode such as MoO₃ (ref. 18). Attractively, this also avoids the use of gold¹⁹. Researchers recently achieved single-junction power-conversion efficiencies of 6% by optimizing the depleted-heterojunction architecture and its constituent materials²⁰.

Enhancing photon absorption from a given amount of colloidal quantum dot film offers significant prospects for increasing the available photocurrent.

Researchers also recently demonstrated the ability to tune the bandgap of a quantum dot film in a tandem cell comprising a visible-absorbing front cell (2 nm diameter nanoparticles) and an infrared-absorbing back cell (4 nm diameter nanoparticles)²¹. The device achieved bandgap control — and thus spectrally selective solar harvesting — solely through quantum tuning. This advance required the development of a composite interlayer that would combine the matched hole current from the front cell and electron current from the back cell, while adding their open-circuit voltages without introducing loss. The tunnel junction of compound semiconductor multijunction cells³ could not be used owing to the lack of degenerate doping in low-temperature-processed transparent conductive oxides. Researchers realized the quantum-tuned tandem cell by using a novel graded recombination layer comprising oxides of different work

functions, from that of the hole-accepting electrode on the front visible-wavelength cell to that of the electron-acceptor on the back infrared-wavelength cell.

Scientists recently proposed that quantum tuning within a single active layer could benefit the performance of solar cells. The resulting quantum funnel cell²² was intended to augment the electron-extracting driving force in the performance-limiting quasi-neutral region by generating a built-in gradient in the conduction band through a quantum-tuned increase in bandgap towards the back of the cell. The principal benefit was realized through the fill factor; in the quantum funnel cell, the bandgap gradient, when positioned to span the quasi-neutral region of the cell at maximum power, ensured that the device remained biased for efficient minority carrier extraction for maximum operating current at the operating voltage.

The future of quantum-tuned solar cells

The electronic properties of colloidal quantum dot films currently limit device performance. To exceed power-conversion efficiencies of 10% in a single-junction planar cell, a material's electron and hole mobility should exceed 10⁻¹ cm² V⁻¹ s⁻¹ and its bandgap should be as trap-free as possible (<10¹⁴ cm⁻³ deep traps)²³. Much progress has been made towards this objective through advances in the packing and passivation of colloidal quantum dots in thin solid films^{20,24,25}.

Novel device architectures have much to offer the field. Nanostructured interfaces at the electron-extracting electrode will enable improved electron extraction by allowing a greater volume of light-absorbing colloidal quantum dot film to be incorporated into a device without compromising the internal quantum efficiency, thus leading to greater overall absorption. This has been demonstrated using a TiO₂ nanostructured electrode infiltrated with colloidal quantum dots²⁶ — known as the depleted bulk-heterojunction solar cell. Much room remains for further improvement through systematically engineering high-electron-mobility electrodes such as nanopillars, nanowires and nanopores.

Enhancing photon absorption from a given amount of colloidal quantum dot film offers significant prospects for increasing the available photocurrent. Nanostructured metals exhibit particularly strong optical scattering, which increases the interaction of light inside the semiconductor relative to today's specular, planar double-pass metals. Plasmonic enhancements, which involve concentrating the optical field in the light absorber, have been exploited in silicon and organic solar cells^{27,28}, and will provide

significant benefits in the quantum-tuned field once suitable-aspect-ratio nanoparticles are tailored to the spectral requirements and the dielectric environment of colloidal quantum dot films.

The urgent need for cost-effective, efficient solar-harvesting solutions creates a powerful motivation for the quantum-tuned photovoltaics community to continue pursuing rapid advances. The scientific disciplines and concepts on which researchers draw are remarkably broad, spanning organic and inorganic materials chemistry and processing, electronic materials transport and trap spectroscopies, and photonic–electronic device engineering. The field's progress so far — and the further advances that are now required — all rely on the interdisciplinary perspective of its growing community of active researchers. □

Edward H. Sargent is at the Department of Electrical and Computer Engineering, Toronto, Ontario M5S 3G4, Canada.

e-mail: ted.sargent@utoronto.ca

References

1. www.eere.energy.gov/solar/sunshot/pdfs/dpw_white_paper.pdf
2. Henry, C. H. *J. Appl. Phys.* **51**, 4494–4500 (1980).
3. King, R. R. *Nature Photon.* **2**, 284–286 (2008).
4. Murray, C. B., Nirmal, M., Norris, D. J. & Bawendi, M. G. *Z. Phys. D* **26**, 231–233 (1993).
5. Yoffe, A. D. *Adv. Phys.* **51**, 799–890 (2002).
6. McDonald, S. A. *et al. Nature Mater.* **4**, 138–142 (2005).
7. Klem, E. J. D., MacNeil, D. D., Cyr, P. W., Levina, L. & Sargent, E. H. *J. Appl. Phys. Lett.* **90**, 183113 (2007).
8. Clifford, J. P., Johnston, K. W., Levina, L. & Sargent, E. H. *J. Appl. Phys. Lett.* **91**, 253117 (2007).
9. Johnston, K. W. *et al. Appl. Phys. Lett.* **92**, 151115 (2008).
10. Johnston, K. W. *et al. Appl. Phys. Lett.* **92**, 122111 (2008).
11. Koleilat, G. I. *et al. ACS Nano* **2**, 833–840 (2008).
12. Luther, J. M. *et al. Nano Lett.* **8**, 3488–3492 (2008).
13. Ma, W., Luther, J. M., Zheng, H., Wu, Y. & Alivisatos, A. P. *Nano Lett.* **9**, 1699–1703 (2009).
14. Debnath, R. *et al. J. Am. Chem. Soc.* **132**, 5952–5953 (2010).
15. Ma, W. *et al. ACS Nano* **5**, 8140–8147 (2011).
16. Pattantyus-Abraham, A. G. *et al. ACS Nano* **4**, 3374–3380 (2010).
17. Liu, H. *et al. Adv. Mater.* **23**, 3832–3837 (2011).
18. Wang, X. *et al. ACS Appl. Mater. Interfaces* **3**, 3792–3795 (2011).
19. Debnath, R. *et al. Appl. Phys. Lett.* **97**, 023109 (2010).
20. Tang, J. *et al. Nature Mater.* **10**, 765–771 (2011).
21. Wang, X. *et al. Nature Photon.* **5**, 480–484 (2011).
22. Kramer, I. J., Levina, L., Debnath, R., Zhitomirsky, D. & Sargent, E. H. *Nano Lett.* **11**, 3701–3706 (2011).
23. Kramer, I. J. & Sargent, E. H. *ACS Nano* **5**, 8506–8514 (2011).
24. Talapin, D. V. & Murray, C. B. *Science* **310**, 86–89 (2005).
25. Lee, J. S., Kovalenko, M. V., Huang, J., Chung, D. S. & Talapin, D. V. *Nature Nanotechnol.* **6**, 348–352 (2011).
26. Barkhouse, D. A. R. *et al. Adv. Mater.* **23**, 3134–3138 (2011).
27. Dionne, J. A., Sweatlock, L. A., Sheldon, M. T., Alivisatos, A. P. & Atwater, H. A. *IEEE J. Sel. Top. Quant. Electron.* **16**, 295–306 (2010).
28. Green, M. & Pillai, S. *Nature Photon.* **16**, 130–132 (2012).

Acknowledgements

E.H.S. acknowledges J. Flexman, I. Kramer and S. Masala for their contributions to the manuscript and figures. This publication is based in part on work supported by award KUS-11-009-21 from the King Abdullah University of Science and Technology, the Ontario Research Fund Research Excellence Program, the Natural Sciences and Engineering Research Council of Canada, and Angstrom Engineering and Innovative Technology.